

Figure 3. Deviation between the calculated and the experimental depolarization ratios for CH_3F plotted as a function of the scaling distance D , for two near-critical isochores with densities $\rho_I = 9132.6 \text{ mol}\cdot\text{m}^{-3}$ and $\rho_{II} = 9190.7 \text{ mol}\cdot\text{m}^{-3}$.

depolarization ratio but the deviation from the calculated value is nearly zero. This indicates the presence of only double scattering processes in this region. In the next region $10^{-3} \text{ m} < D < 10^{-2} \text{ m}$, however, there is a sharp increase in the deviation which is due to higher order contributions since according to (4) and (10), one has $I_{\text{dep}}^{(3)}/I_{\text{pol}}^{(1)} \approx D^{-2}$ and $\Delta_{(3)}^m \approx aD^{-1} + bD^{-2} + \dots$, a, b, \dots being the coefficients which depend on the scattering geometry. And finally, as one approaches very close to the critical point, the

gravity-induced density gradients become increasingly important for which there is again a sharp increase in the deviation of opposite sign between the calculated and observed values of $\Delta \cdot z^{-1}$.⁹ In this region, there is also the influence of the Ornstein-Zernike factors present in expression 4.

It is interesting to compare the present results for CH_3F with those for Xe and CO_2 obtained previously in this laboratory.⁴ This comparison is also shown in Figure 2. It is clear that the behavior of the $\Delta \cdot z^{-1}$ versus D plots in the critical region is similar for all the three fluids studied up till now. Although it appears from this comparison that the observed depolarization ratio increases as one goes down in the molecular anisotropy of the fluid, this may also be due to the error in the determination of the optimum height z as well as due to the uncertainty in the values of the critical point parameters used in the calculation of the scaling distance D . For instance, a small increase in z , in the order of its accuracy for the results of Xe, or the use of recent values for the critical point parameters¹⁰ for CO_2 gives much less deviations than those shown in Figure 2.

Acknowledgment. We thank Dr. A. C. Michels for many helpful discussions and Mr. N. Blom for preparing the drawings. This is the 380th publication of the Van der Waals Laboratory.

Registry No. CH_3F , 593-53-3.

(9) Hohenberg, P. C.; Barmatz, M. *Phys. Rev.* **1972**, *A6*, 289-313.

(10) Sengers, J. V.; Levelt Sengers, J. M. H. *Annu. Rev. Phys. Chem.* **1986**, *37*, 189-222.

Picosecond Phase Conjugate Reflectivity of Gold Colloids by Degenerate Four-Wave Mixing

T. Dutton,[†] B. VanWanterghem, S. Saltiel,[‡] N. V. Chestnoy,[§] P. M. Rentzepis,*

Department of Chemistry, University of California, Irvine, California 92717

T. P. Shen, and D. Rogovin

Rockwell International Science Center, Thousand Oaks, California 91360 (Received: May 22, 1989; In Final Form: September 21, 1989)

We measure the efficiency and phase of picosecond phase conjugate reflectivity by degenerate four-wave mixing for colloidal gold suspended in water and in glass. Evidence is found for extremely high $\chi^{(3)}$ for the gold particles. However, the efficiency has a power dependence which is not increasing quadratically with pump energy. Small-scale lensing effects become significant at high pump energies. Additionally, both the glass-based and the water-based colloids show a visible "permanent" bleaching effect after absorbing only a few pulses of GW/cm^2 intensity.

Introduction

In the field of nonlinear optics, there is currently a great deal of interest in semiconductor and metal colloidal suspensions in liquid and solid media. These suspensions hold promise, from the applications perspective, since extremely high optical nonlinearities are associated with them.¹⁻³ While they lack the efficiency of materials such as photorefractives, they have two advantageous characteristics. First, they have an extremely fast response, on the order of picoseconds, and second, the optical nonlinearities of these suspensions are due almost entirely to the suspended particles, which comprise a volume fraction of only about

10^{-6} – 10^{-4} . Below the pump intensity region where saturation effects become significant, our own unpublished data indicate that the reflectivity of the gold colloid liquid is ~ 1000 times less than that of CS_2 . Starting from one of the simplest equations for phase conjugate reflectivity (R)

$$R \sim \tan^2(KL)$$

where K is defined as the nonlinear coupling coefficient (K is proportional to $\chi^{(3)}$ times the field intensity) and L is the interaction length, we consider the low-conversion (low-reflectivity) limit. In this region, the phase conjugate (PC) reflectivity is

[†] Department of Physics, University of California at Irvine.

[‡] Permanent address: Department of Physics, Sofia University, Sofia-1126, Bulgaria.

[§] Permanent address: School of Medicine, University of California at San Francisco, San Francisco, CA 94117.

(1) Nasu, H.; Mackenzie, J. D. *SPIE Opt. Eng.* **1987**, *26*, 102-106.

(2) Hache, F.; Ricard, D.; Flytzanis, C. *J. Opt. Soc. Am. B* **1986**, *3*, 1647-1655.

(3) Heilweil, E.; Hochstrasser, R. M. *J. Chem. Phys.* **1985**, *82*, 4762-4770.

proportional to the square of K , and we can equate the approximations for CS_2 and gold colloid samples, correcting for the reflectivity difference between the two and the actual volume fraction ($\sim 4 \times 10^{-6}$) for the gold colloid:

$$R_{\text{Au colloid}} = R_{\text{CS}_2} \times 10^{-3}$$

or

$$(K_{\text{Au}}L_{\text{eff}})^2 = (K_{\text{CS}_2}L)^2 \times 10^{-3}, \quad \text{where } L_{\text{eff}} = (4 \times 10^{-6})L$$

We find, after the substitutions

$$K_{\text{Au}} = (1.6 \times 10^{-8})^{-1/2} K_{\text{CS}_2}$$

or, equivalently, that the $\chi^{(3)}$ of the gold particle is $\sim 10^4$ times that of CS_2 . For the current, in-depth theoretical treatment, see ref 4. The PC reflectivity of the matrix is insignificant at low intensities but becomes comparable to that of the particles at higher intensities because of a saturation of the nonlinear susceptibilities of the particles. Thus, the suspension may be "tailored" to vary the total optical nonlinearity in the sample.

In this paper, we discuss some of the linear and nonlinear properties of gold colloidal suspensions based on CW absorption and picosecond optical phase conjugation measurements.

Experimental Section

Two types of gold colloid samples were used, a water-based colloid, prepared following the method of Turkevich,⁵ and a solid glass-based sample obtained from Schott glass (sample type RG-6, 1-mm thickness). The water-based colloid had a local absorbance maximum due to surface plasmons on the gold particles, measured by a Cary 219 spectrophotometer, of 1.20 cm^{-1} at 519 nm (sample thickness of 2 mm). Similarly, the absorbance of the Schott RG-6 glass had a local maximum of 4.00 cm^{-1} at 535 nm. This was superposed on a background absorbance, due to interband transitions, which becomes noticeable at $\sim 620 \text{ nm}$ and increases in magnitude as wavelength decreases. The width of the peak for the local maximum was approximately 100 nm for both samples before bleaching. Bleaching consisted of extended exposure (several hundred mJ/cm^2) of the liquid colloid in a 2-mm static cell with intermittent agitation so as to achieve uniformity throughout the sample. This was required for accurate absorbance measurements carried out later in the spectrophotometer. After bleaching, the width could not be estimated accurately for the liquid and postexposure absorbance measurements could not be made at all for the RG-6 glass due to the very small size of the irradiated spot.

Optical phase conjugation measurements were made in two different pump intensity regions. The phase of the nonlinear susceptibility was measured by means of a nonlinear interferometer, described elsewhere.⁶ A semiconductor colloid glass, whose $\chi^{(3)}$ (both magnitude and phase) was previously determined, was used in one arm as a reference and a gold colloid sample, whose phase was to be determined, was placed in the other arm. The interferometer operated at a wavelength of 532 nm via a CW mode-locked laser providing 1200 mW of average power at a repetition rate of 82 MHz. The peak intensities at the sample were $\sim 1\text{--}2 \text{ kW}/\text{cm}^2$.

Since the phase conjugate reflectivities of most high-speed (i.e., picosecond response) materials are very low at the low peak intensity levels of CW mode-locked lasers (a few kilowatts per square centimeter), scattering is comparable to the PC reflectivities of $\sim 10^{-10}\text{--}10^{-9}$. For this reason, a lock-in amplifier was used in addition to a series of diaphragms to reject scattered light.

A pulsed Nd:YAG laser operating at 2 Hz and 532 nm was used for the high-intensity PC reflectivity measurements (see Figure 1). A passively mode-locked oscillator was followed by

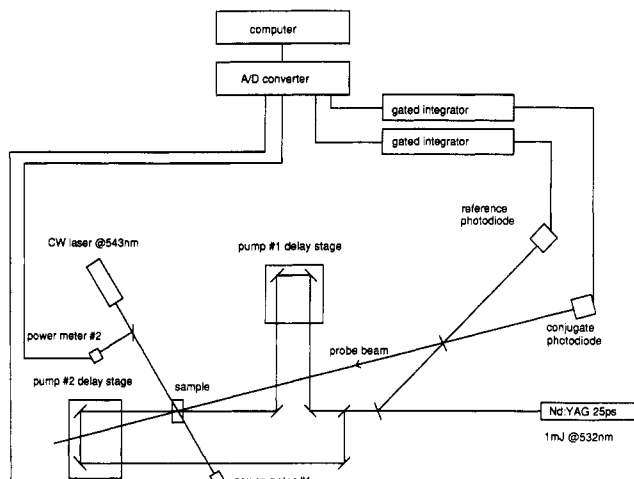


Figure 1. Laser system for high-intensity, picosecond DFWM experiments.

a pulse selector, two amplifier stages, and a frequency-doubling crystal. This provides a 25-ps, 532-nm pulse with a diameter of $\sim 2 \text{ mm}$ and energies ranging from a few tens of microjoules to a few millijoules. This pulse is split into four components. Two counterpropagating pump beams and one weaker probe beam are arranged in the counterpropagating degenerate four-wave mixing (DFWM) geometry. The fourth component is used as a reference signal. The reference signal as well as the phase conjugate signal is detected by high-voltage vacuum photodiodes; diaphragms are used to minimize extraneous light. These are scanned by gated integrators at a 4-ns gate width (long enough to allow for trigger jitter and short enough to minimize detector of stray light). These integrators, in turn, are monitored with a computer interface (A/D conversion), and ultimately the data are manipulated by a DEC microvax computer.

The water-based colloid suspension was studied both in a static, closed cell and in a flowing cell in circuit with a 200- cm^3 reservoir. The flowing cell arrangement was used in cases where we wished to minimize the influence of sample deterioration during reflectivity measurements, while the static cell was used for absorption band measurements before and after sample decomposition.

During some experiments, the bleaching of the gold colloid glass was monitored by measuring the absorbance in the sample at a wavelength of 543 nm. This wavelength is well within the absorption resonance of the colloids and is conveniently provided by a 1-mW continuous wave HeNe laser. The laser intensity transmitted through the four-wave mixing region in the sample was measured by a photodiode, as well as a reference signal. Thus, this system could monitor the influence of each successive laser pulse on the absorption of the gold colloid sample. We assumed that our absorption monitor at 543 nm was approximately indicative of absorbance changes at 532 nm, the wavelength at which our phase conjugation experiments were carried out.

Results

Data from the high-energy, pulsed YAG laser for gold colloid glass and water suspensions provided a power dependence of the phase conjugate reflectivity for intensities ranging up to a few GW/cm^2 (Figures 2 and 3a). In our initial studies the probe beam power was $\sim 10\%$ of the pumps, and in later experiments it was adjusted to be 50% of the pump power. We did not detect any qualitative difference (due to the probe/pump ratio change) in the structure of the measured reflectivity power dependence. At these low overall reflectivities, we did not expect any influence of pump depletion since a probe intensity comparable to a pump still would drain the pump by only 0.1%.

Our data for the water-based suspension indicate that the reflectivity does not vary significantly with pump intensity in the region of $\sim 500 \text{ MW}/\text{cm}^2$. This does not mean that the PC reflectivity is constant but rather that it does not vary strongly and certainly does not vary quadratically with the pump intensity

(4) Hache, F.; Ricard, D.; Flytzanis, C.; Kreibig, U. *Appl. Phys. A* **1988**, *47*, 347-357.

(5) Turkevich, J.; Stevenson, P.; Hillier, J. *Faraday Discuss. Chem. Soc.* **1951**, *11*, 55.

(6) Saltiel, S.; VanWanterghem, B.; Rentzepis, P. M. *Opt. Lett.* **1989**, *14*(3), 183-185.

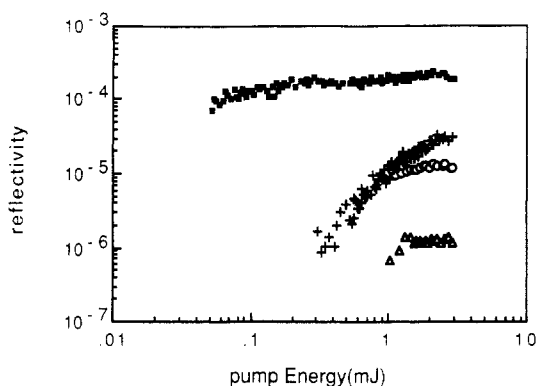


Figure 2. Phase conjugate reflectivity of Schott RG-6 gold colloid glass for high pump intensity, probe/pump ratio = 0.1, low repetition rate, 25-ps pulses for all beams incident (■), pump 1 blocked (○), pump 2 blocked (△), and all beams incident on an undoped glass sample (+). The flat response for gold glass is largely due to the formation of permanent gratings in the sample. All beams are linearly copolarized.

as would be expected for a PC process.

For the water suspension, some experiments indicated a "flat" spot or local maximum in the intensity dependence at a pump energy of a few hundred microjoules (corresponding to intensities of a few hundred MW/cm²). At higher pump intensities, the reflectivity begins to rise again as a function of pump intensity. It is difficult to specify this power dependence analytically since, in our pump energy range, the slopes of the curves vary continuously on a logarithmic scale, but the range is not large enough to assign an exponential power dependence. At first glance, these power dependence curves do not display characteristics that would be associated with the usual approximations⁷ (i.e., "tangent squared" and similar power dependences). These results will be discussed below.

During exposure to the high-power pulsed laser, the Schott RG-6 glass gold colloidal suspension developed permanent gratings which caused the "phase conjugate" reflectivity to remain approximately constant over a wide pump beam energy range. One partial explanation for this result is the possibility of significant particle decomposition in the regions of the antinodes of the optical standing waves. Thus, the total diffraction grating would be the sum of the linear gratings formed by sample damage and the nonlinear gratings which still exist at the nodes of the optical standing waves. If we assume the linear contribution to dominate in our experiment, we would expect constant reflectivity. Interestingly, the total phase conjugate signal is significantly greater than the sum of the two "separate" permanent gratings, i.e., the signals detected when one or the other of the pump beams was blocked. This implies the dominance of the nonlinear contribution, in direct contradiction to our initial premise. A hand-waving solution is to say that the nonlinear solution dominates with saturation of the nonlinearity being the crucial factor in the case of all beams incident on the sample.

There was also a permanent change in the absorption of the colloids, both liquid and solid (Figures 4 and 5), upon exposure to the high-power pump pulses. This appeared as a "bleaching" of the colloid or occasionally the appearance of a pale bluish spot. These changes appeared to be permanent. Our data from the CW spectrophotometer confirmed this; absorbance dropped in the blue and increased in the red wavelength region.

We measured the change in absorbance in the Schott RG-6 filter, as a function of total laser exposure upon the sample spot, for two different average laser pulse energies, 0.1 and 1.0 mJ (Figure 4). Note that, upon interrogation by 1-mJ pump pulses, the absorbance at 543 nm has permanently dropped from 0.41 to 0.3 after only a few millijoules of accumulated energy. For the same total laser energy exposure, the lower energy pulses have done far less damage. The most extreme case, namely, irradiation

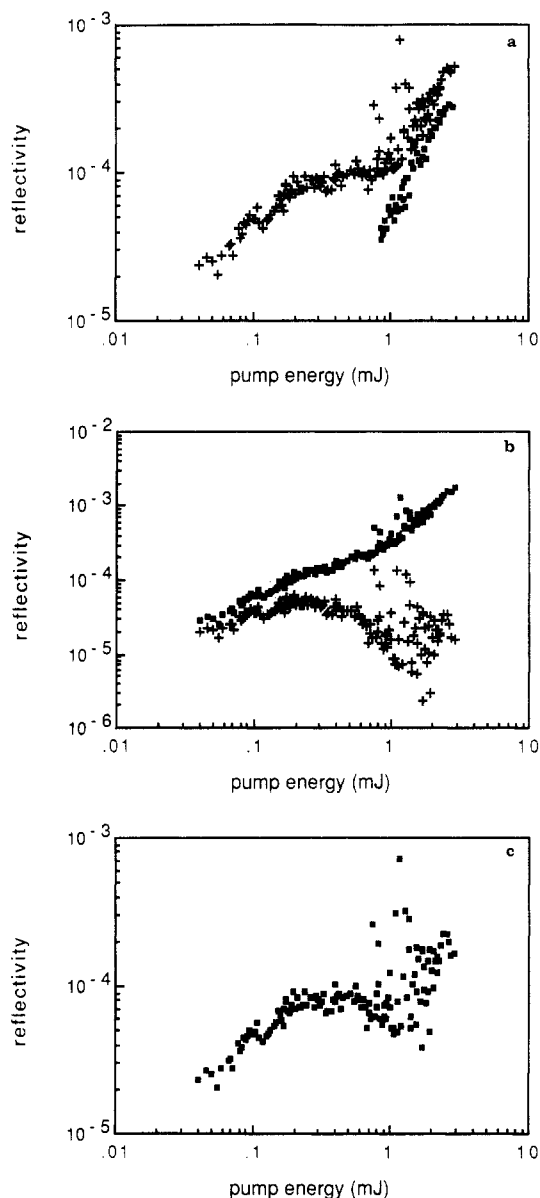


Figure 3. (a) Phase conjugate signal for water-based gold colloid (+) and plain water (■) in a 2-mm flow-through cell. (b) PC reflectivity if the signal from the water and cell is assumed in phase (+) and antiphase (■) with that of the gold particles. (c) PC reflectivity when water and cell nonlinearities are assumed to be real and those of the gold particles are assumed to be imaginary. All beams are linearly copolarized.

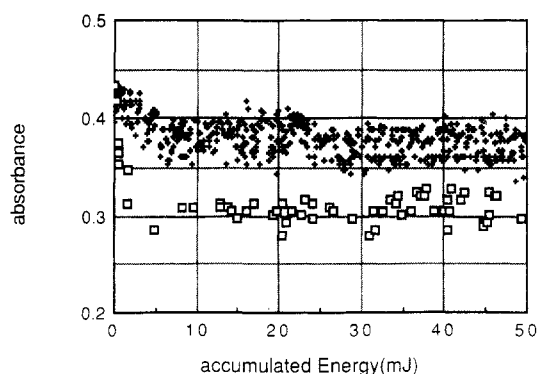


Figure 4. Change in optical absorbance at $\lambda = 543$ nm of Schott RG-6 as a function of total energy flux from pulsed Nd:YAG laser ($\lambda = 532$ nm) for average pulse energies of 0.1 mJ/pulse (+) and 1.0 mJ/pulse (□).

(7) Jian-quan, Y.; Guosheng, Z.; Siegman, A. E. *Appl. Phys. B* **1983**, *30*, 11-18.

with a few hundred mJ/s from the CW mode-locked Nd:YAG laser, did not result in any change in absorbance although the

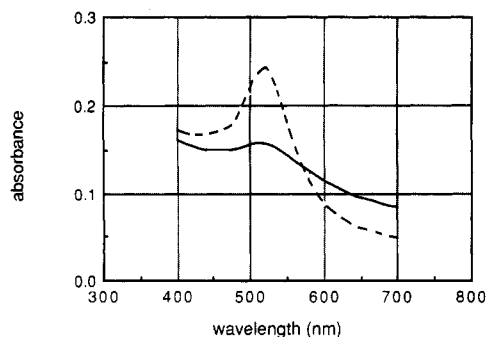


Figure 5. CW absorbance of water-based gold colloid in a 2-mm cell before (---) and after (—) sample damage.

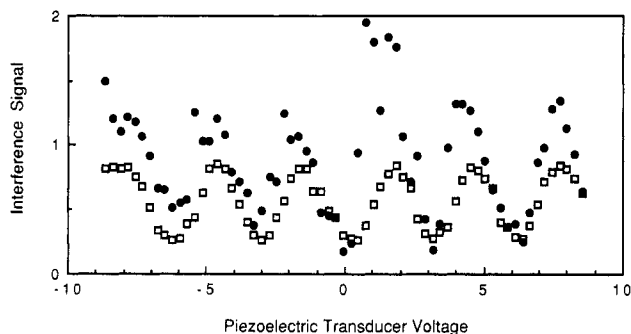


Figure 6. A comparison of the interference of conjugate signals (●) and reference signals (□) from Schott RG-6 gold colloid glass and Schott OG-530 semiconductor colloid glass as a function of delay in the arm of the nonlinear interferometer. Since the phase of the PC signal from OG-530 is known to be negative and real in this region, the phase of RG-6 must be the same.

accumulated energy was many orders of magnitude larger than the pulsed laser provided.

At the highest pulse energies, there was also an increase in the far field of phase conjugate spot size; the transmitted probe pulse showed a similar phenomenon. Since the transmitted probe pulse shares this "bloomed" appearance (generally appearing as a somewhat distorted series of concentric rings) in the far field, the most probable cause of the phase conjugate "bloom" structure is that it is an accurate replication of the self-focusing or -defocusing of the probe signal. That this phenomenon occurs at high intensities is expected; the self-focusing or self-defocusing phenomenon is also due to the third-order nonlinear susceptibility. We neglect the possibility of thermal lensing since the entire phase conjugate interaction is completed within roughly 50 ps and the time between successive pulses is 500 ms.

Figure 6 shows phase conjugate signal interference and pump signal interference from Schott RG-6 gold colloid glass and Schott OG-530 semiconductor colloid glass as a function of the change in path length of one arm of the interferometer (measured by voltage on a piezoelectric transducer). The path length changes are necessarily on the order of the optical wavelength and are not to be confused with "macroscopic" path length delays associated with lifetime measurements. Since the maxima and minima of the two signals coincide and we have measured the phase of $\chi^{(3)}$ of the Schott OG-530 to be negative and real (data to be published elsewhere) for the CW mode-locked laser's frequency, intensity (2 kW/cm^2), and repetition rate, we determined that, for these parameters, the phase of the total third-order nonlinear susceptibility for the gold colloid sample is negative and real. In other words, for $\chi^{(3)} = \chi_{\text{real}} + i\chi_{\text{imaginary}}$, it was determined that the effective $\chi_{\text{imaginary}}$ is negligible compared to χ_{real} and that χ_{real} is negative. Since the colloid sample is actually a composite system, we cannot attribute this $\chi^{(3)}$ to the particles without further assuming that the nonlinear susceptibility of the glass matrix is insignificant compared with that of the gold particles at this power level. Evidence supporting this claim is that a plain glass sample of 1-mm thickness did not provide a detectable phase conjugate signal when pumped by the CW mode-locked laser of the modified

Twyman-Green (TG) interferometer. Therefore, we attribute the negative and real nonlinear susceptibility to the gold particles.

Discussion

Upon laser irradiation, surface plasmons, other intraband transitions, and interband transitions are excited on the gold particle. Surface plasmons on a uniform sphere have their resonance frequency related to the bulk plasma frequency⁸ in the first approximation by

$$\nu_{\text{sp}} = \nu_{\text{bulk}}(L/(2L + 1))^{1/2} \quad L = 1, 2, 3, \dots$$

or

$$0.58\nu_{\text{bulk}} < \nu_{\text{sp}} < 0.71\nu_{\text{bulk}}$$

For gold, $\nu_{\text{bulk}} = 2 \times 10^{15} \text{ Hz}$, so the dipole surface plasmon frequency is $1.16 \times 10^{15} \text{ Hz}$. The actual absorption resonance for gold particles in a dielectric is shifted according to the refractive index of the medium. For our water and glass matrices, this results in a resonance in the visible region, a typical value for the position of the peak being $\lambda = 520 \text{ nm}$. The most obvious manifestation of the interband transitions is the yellow appearance of bulk gold under ambient light.

Our phase measurements on the CW mode-locked system indicated that a negative and real nonlinear susceptibility dominated at these high pulse repetition rates and low (kW/cm^2) peak pump intensities. A negative and real susceptibility is characteristic of a thermal grating and is attributed to local heating resulting from plasmon decay or interband transitions via nonradiative channels. Since thermal diffusion through the colloid is slow compared to our 82-MHz repetition rate, the phase grating builds after a number of laser pulses have passed through the sample and a thermal equilibrium is established. There are purely electronic contributions to the nonlinear susceptibilities such as the nonlinear electronic polarizabilities and the saturation of interband transitions,^{2,9} but these are expected to be very weak at these low peak intensities. We would expect these effects to be dominant only during spatial and temporal overlap of the pulses since the electronic hyperpolarizabilities decay in much less than a picosecond.

It is interesting to do a simple calculation to consider how much energy might be absorbed by each gold particle in the liquid suspension.

A water-based colloid solution contains approximately 74 mg of gold per liter of water. Since the density of gold is 19.3 g/cm^3 , this corresponds to a total volume of $4 \times 10^{-3} \text{ cm}^3$ or a volume fraction ($\text{vol}_{\text{gold}}/\text{vol}_{\text{total}}$) of approximately 4×10^{-6} . Typical values for the radius of the gold spheres in such solutions range from ~ 40 to $\sim 120 \text{ \AA}$, corresponding to sphere volumes between 2.7×10^{-19} and $7.2 \times 10^{-18} \text{ cm}^3$. Electron micrographs indicated that particles in our solutions had an average radius of 120 \AA . This is equivalent to a number of spheres per liter ranging from 1.5×10^{16} to 5.6×10^{14} .

If our laser beam diameter is 2 mm and our sample thickness is 2 mm, then the volume of colloid interrogated is $8 \times 10^{-3} \text{ cm}^3$. Equivalently, our beam interacts with 1.2×10^{11} spheres (assume 40- \AA -radius particles) or 4.5×10^9 spheres (assume 120- \AA -radius particles). Since the absorbance or, equivalently, the extinction is approximately 0.3 and this is almost exclusively true absorption for particles of this size (the remainder being scattered), we can say that half of the incident photons are absorbed by the gold spheres. We consider absorption by the water to be negligible.

So if the power irradiated on the sample in the CW mode-locked case is 100 mW (at 82 MHz), then 1.35×10^9 photons are absorbed by 1.2×10^{11} or 4.5×10^9 spheres. So, for the case of the larger spheres, one photon is absorbed by every third sphere in one laser pulse. It is not surprising, then, that in this intensity region cumulative thermal effects would dominate the four-wave interaction.

In the case of the millijoule pulse, that is not at all the case. Either 4.6×10^4 or 1.2×10^6 photons are absorbed per sphere

(8) Kittel, C. *Solid State Physics*; Wiley: New York, 1987.

(9) Johnson, P. B.; Christy, R. W. *Phys. Rev. B* 1972, 6, 4370-4379.

if the low-intensity absorbance were to scale to high intensities. This is equivalent to either 1.8×10^3 or 4.8×10^4 (photons/particle)/ps during laser irradiation. Remember that the smaller (40-Å radius) particle consists of $\sim 4 \times 10^3$ atoms while the larger (120-Å radius) particle consists of $\sim 10^5$ atoms. Before discussing the characteristics of the optical nonlinearities associated with the millijoule (GW/cm²) laser pulses, we will consider the results of our sample damage experiments.

We know from our measurement of absorbance changes that, for pulse energies of ~ 0.1 mJ, the material begins to decompose; the rose color of the solution disappears after only a few pulses. This level of irradiation corresponds to absorption of either 180 (photons/particle)/ps (40-Å-radius sphere) or 4.8×10^3 (photons/particle)/ps (120-Å-radius sphere). If each photon contains 2.3 eV of energy and the specific heat for bulk gold at room temperature is 0.126 J/(g K), then the temperature rise associated with the smaller (5.2×10^{-18} g) sphere and the larger (1.4×10^{-16} g) sphere after 1 ps at 1-mJ pump energies would be about 1000 °C, approximately the melting temperature of gold. By this point, a significant decrease in the absorbance should occur due to a saturation of interband and intraband transitions.² If the absorbance did not decrease, then after the entire pulse has passed through the sample, a significant fraction of the gold particles would be melted. (The heat of melting of gold is ~ 12 kJ/g-mol.) This temperature rise added onto the ambient temperature obviously means that the temperature at the surface of the spheres is far above the boiling point of the solvent water.

In discussing the evolution of the particles' decomposition, we should also investigate quantum mechanical considerations such as photoionization at these intensities. In the case of ionization, we must determine whether the dominant feature of the laser pulse's nonlinear interaction with the particle is the field strength, E , or the energy per photon. Typically, a Keldysh parameter¹⁰

$$\gamma = (\omega/eE)(m\Delta)^{1/2}$$

(where ω is the laser frequency, Δ is the energy gap (or ionization potential), E is electric field strength of the pulse, and e and m are the charge and mass of an electron) is used to determine which feature is dominant. For $\gamma \gg 1$, multiphoton effects are dominant while for $\gamma \ll 1$, the field strengths are more important. The ionization potential for atomic gold is 9.22 eV while the work function for bulk gold is about 5.3 eV. We would expect the small gold sphere to have an "ionization potential" somewhere between these two values, probably much closer to the work function since clusters consisting of an excess of 10^3 atoms are considered to have bulk properties.¹¹ We expect that this work function might be further decreased due to plasma-induced screening. (Recall that interband transitions in gold are significant for photon energies exceeding 2 eV.⁶) For our experimental conditions, this corresponds to the parameter $\gamma > 100$. Therefore, we would expect the influence of multiphoton absorption to dominate the nonlinear photoionization rather than the effect of field strength on tunneling.

For this reason, the ejection of electrons into the adjacent matrix by means of multiphoton absorption or plasma screening enhanced (thermionic) one-photon absorption is likely to occur, thus complicating the melting of the gold particles and the boiling of the solvent water.

If there are 5.6×10^{14} 120-Å-radius particles per liter of solvent, then there is a center-to-center distance between nearest neighbors of $\sim 2.4 \times 10^4$ Å. This is approximately 100 times the particle size so we would expect that the degradation of the colloid to be due to a breaking up of the particles rather than aggregation. This conclusion, in conjunction with our spectrophotometer results (Figure 5), confirms the results of Ascarelli and Cini¹² that there is a red shift in the absorption resonance as particle size decreases. Our resonances appear broadened since our sample was liquid,

and therefore damaged and undamaged regions were mixed, i.e., a broader size distribution.

The high-intensity optical nonlinearities of the particle are also changed during excitation due to the interband transition induced free carriers. The refractive index should change due to an increase in the electron density. The plasma resonance should shift to higher energy since it increases as the square root of conduction electron density, although this is partially compensated for by broadening due to a temperature increase.

It is difficult to determine the intensity dependence of the gold sphere's hyperpolarizability without knowing the relative phases of the nonlinear susceptibility of the water or glass matrix and the gold particles. We know the relative magnitude of $\chi^{(3)}$ for these matrices (see, for example, Figure 3a); the phase should be positive and real for the water, quartz, and glass.¹ We know that the signal of a glass sample is comparable to the signal from the colloid sample at intensities above 1 GW/cm²; therefore, the functional form is strongly dependent on the assumed phase relationship of the nonlinearities of the gold particles and the solvent (see Figure 3b,c).

We do not necessarily expect the nonlinear susceptibility in the 2-Hz, GW/cm² intensity experiments to have the same phase as the CW mode-locked experiments. Thermal gratings dominate the nonlinearities in the low peak intensity, high repetition rate CW mode-locked laser system, since the time scale for heat diffusion throughout the colloid allows for cumulative (with respect to the number of mode-locked laser pulses) nonlinear optical effects; single-pulse nonlinearities are too weak at these peak intensities to be detected.

Brorson et al.¹³ have measured heat transport in metal films and found heat to propagate at roughly the Fermi velocity, indicating that thermal effects equilibrate very quickly within the confines of the metal itself. Nunzi et al.¹⁴ have measured picosecond phase conjugation in metallic films and found thermal effects to dominate at high intensities, while other researchers have actually measured the phase of the susceptibility of metallic colloids in the 100 MW/cm² region and found it to be primarily imaginary.^{2,4}

The measurements referenced above are problematic since thermal effects, although obviously the result of absorption, result in a *phase* grating, corresponding to a *real* $\chi^{(3)}$, while an imaginary $\chi^{(3)}$ corresponds to an *absorptive* or *amplitude* grating. Our own pump delay data (unpublished) on gold colloids indicate a decay time of only a few picoseconds or less. It is possible that the grating is a thermal phase grating which transfers its heat to the matrix on a time scale of a few picoseconds. If we assume that the change in refractive index with respect to temperature ($\partial\chi^{(3)}/\partial T$) is much smaller in the matrix than in the metal particles, then we cannot exclude the possibility of a thermal grating in our high-intensity experiments.

We could resolve the phase discrepancies by assuming that the instantaneous grating created during the four-wave interaction is an absorptive grating (imaginary $\chi^{(3)}$), which *after* excitation is effectively a thermal grating until the excited gold particle transfers its excess energy to the matrix. This result assigns a complex phase for $\chi^{(3)}$ and allows the possibility of a resolution of conflicting reports.^{4,14} We plan to carry out our own phase measurements at high intensities via interferometric methods analogous to our low-intensity method.⁶

If we assume that the phase remains imaginary throughout our intensity range (100 MW/cm²–3 GW/cm²), then the experimental results, after subtraction of the solvent signal (Figure 3c), indicate an apparent saturation of one component of the nonlinearity at ~ 500 MW/cm², confirming the results of Hache et al.² At the highest intensities, from 0.8 to 3.0 mJ, this data shows an apparent decrease in the signal-to-noise ratio. This may be attributed to one or more of several possible causes, such as sample inhomogeneity, damage during irradiation, or competition of self-fo-

(10) Keldysh, L. V. *Sov. Phys.—JETP (Engl. Transl.)* **1965**, 20 (5), 1307–1314.

(11) Kreibitz, U. In *Growth and Properties of Metal Clusters*; Elsevier: New York, 1980.

(12) Ascarelli, P.; Cini, M. *Solid State Commun.* **1976**, 18, 385–388.

(13) Brorson, S. D.; Fujimoto, J. G.; Ippen, E. P. *Phys. Rev. Lett.* **1987**, 59 (17), 1962–1965.

(14) Nunzi, J. M.; Ricard, D. *Appl. Phys. A* **1984**, 35, 209–216.

cusing and self-defocusing elements of the total nonlinear susceptibility. The noise is partially an artifact of the method of subtraction of the solvent's conjugate signal. For example, if we subtract, point by point, our data from a hypothetical $y = Ax^2$ representing the conjugate signal of the solvent in a region where the solvent signal is $\sim 1/2$ of the total signal, our apparent signal-to-noise ratio decreases by a factor of 2. This effect is even more pronounced in the case where the particle signal is assumed in phase with the solvent signal (see Figure 3b). For this reason, it is difficult to say with certainty whether the saturation of the reflectivity in the 1-mJ pump energy region is total or partial. However, it should be noted that there was a significant variation in the conjugate signal's far-field transverse spot size and structure, as observed pulse by pulse, which could result in a variation in the amount of light collected by the detectors.

If the $\chi^{(3)}$ of the gold particles is due to more than one physical mechanism or if there is a nonlinear interaction between the particles and the solvent, then the phase may be intensity dependent. A mechanism dominant at low intensities may saturate at higher intensities resulting in the dominance of another mechanism and a possible change in phase. A complete determination of this functional dependence would clarify the dynamics of the nonlinear properties of gold spheres. It is already evident that the nonlinear susceptibility is huge for these particles. The

phase conjugate reflectivity for pumping Au colloidal suspensions with less than 100 μJ is comparable with that of CS_2 , currently the standard of high-speed highly nonlinear materials. Given that the volume fraction is $\sim 4 \times 10^{-6}$, this indicates a nonlinear susceptibility for gold particles which is ~ 4 orders of magnitude higher than that for CS_2 .

Conclusions

We have determined experimentally the intensity dependence of the picosecond phase conjugate reflectivity in gold colloids for pump intensities on the order of 1 GW/cm^2 , investigated the intensity dependence of sample damage, and determined the phase of the nonlinear susceptibility of gold colloids via interferometric methods using a CW mode-locked Nd:YAG laser and have also recognized the significance of the phase relationship of the nonlinear susceptibilities in a multicomponent system. This is significant in an applications environment since the functional intensity dependence could have its shape "tailor-made" by adjusting the stoichiometry of the constituents.

Acknowledgment. This research has been supported by the Air Force Office of Scientific Research Grant F29601-87-K0057 and by Rockwell International Corp. Grant B8X197858.

Registry No. Au, 7440-57-5.

Ultraviolet and Visible Charge-Transfer Absorption and Emission Spectra of Some Polar Dyes in Aqueous Solution under High Pressure¹

Lorrie Comeford and Ernest Grunwald*

Chemistry Department, Brandeis University, Waltham, Massachusetts 02254 (Received: June 1, 1989; In Final Form: October 6, 1989)

The ultraviolet and visible absorption and emission spectra of aqueous solutions of four dyes, 4-amino-4'-cyanobiphenyl, carbostyryl 124, coumarin 1, and coumarin 102, and the absorption spectrum of 4-nitroaniline were measured at pressures up to 6 kbar. The compressions produced red shifts or, in one case, virtually no shifts. The variations of ν_{max} with pressure were reproduced by linear equations. The largest red shift was for the absorption of 4-nitroaniline, where the slope was $-107 \text{ cm}^{-1}/\text{kbar}$. The slopes for the two coumarin dyes were remarkably different, considering the similarity of their structures. Established theory of dielectric solvation effects on Franck-Condon transition energies was modified to apply to solvents of high dielectric constant and predicted pressure effects whose magnitude is small compared to observation. A quasi-thermodynamic approach was more encouraging. Because the charge-transfer excited states are zwitterions, the hypothetical excitation process at equilibrium is attended by a large decrease in volume due to electrostriction of the solvent. Thus there is marked volume strain in the Franck-Condon final state. The decrease in volume was estimated for three of the substrates and accounts for a major part of the pressure shifts.

Medium effects on electronic transition energies have long been used as probes for solvation energies.²⁻⁴ Especially useful have been the intramolecular charge-transfer transitions $\text{D-R-A} \rightarrow \text{D}^+-\text{R-A}^-$ and their reverse, where the symbols D and A denote an electron donor and acceptor group, and R denotes an intermediate structure which provides a resonance pathway.^{5,6} Such transitions produce large changes in polar character as the polar substrate D-R-A changes to a zwitterion $\text{D}^+-\text{R-A}^-$ whose electric dipole consists of two discrete monopoles. Moreover, London dispersion interactions with solvent are also relatively large, especially when the resonance pathway is long⁷ (as in merocyanine

dye molecules, for example), and hydrogen-bonding solvation can be significant, especially when the groups D and A are exposed to solvent.

In this paper we report the effect of pressure on charge-transfer transition energies for five substrates in aqueous solution at 25 °C. The substrates are 4-amino-4'-cyanobiphenyl (I), carbostyryl 124 (II), coumarin 1 (III), coumarin 102 (IV), and 4-nitroaniline (V); structural formulas are given in Scheme I. Pressures range up to 4-6 kbar, in which range there are substantial changes in water properties. At 25 °C, between 1 atm and 5 kbar, the liquid density increases by 15.2%,⁸ the dielectric constant by 18.8%,⁹ and the refractive index by 3.8%.¹⁰ Substrates I-IV were measured both in absorption and emission, while 4-nitroaniline could be measured only in absorption. The latter substrate pro-

(1) Dedicated to Professor Harry Drickamer on the occasion of his 70th birthday and retirement.

(2) Scheibe, G.; Bruck, D. Z. *Elektrochem.* **1950**, *54*, 403.

(3) Kosower, E. M. *J. Am. Chem. Soc.* **1958**, *80*, 3253, 3261, 3267.

(4) Kamlet, M. J.; Abboud, J. L. M.; Taft, R. W. *Prog. Phys. Org. Chem.* **1981**, *13*, 485.

(5) (a) Dimroth, K.; Reichardt, C.; Siepmann, T.; Bohlmann, F. *Liebigs Ann. Chem.* **1963**, *661*, 1. (b) Reichardt, C.; Harbusch-Goernert, E. *Ibid.* **1983**, *5*, 721. (c) Tamura, K.; Imoto, T. *Bull. Chem. Soc. Jpn.* **1975**, *48*, 369.

(6) Buncl, E.; Rajagopal, S. *J. Org. Chem.* **1989**, *54*, 798.

(7) (a) Grunwald, E.; Price, E. *J. Am. Chem. Soc.* **1964**, *86*, 4517. (b) Grunwald, E.; Fong, D.-W. *J. Phys. Chem.* **1969**, *73*, 3909.

(8) Grindley, T.; Lind, J. E. *J. Chem. Phys.* **1971**, *54*, 3983.

(9) (a) Lees, W. L. Ph. D. Thesis, Harvard University, 1949. (b) Sciafe, B. K. P. *Proc. Phys. Soc. London* **1955**, *B68*, 790. (c) Srinivasan, K. R.; Kay, R. L. *J. Chem. Phys.* **1974**, *60*, 3645.

(10) Vedam, K.; Limsuan, P. *J. Phys. Chem.* **1978**, *69*, 4772.